How does the SST variability over the western North Atlantic Ocean control Arctic warming over the Barents–Kara Seas?

2017 Environ. Res. Lett. 12 034021

(http://iopscience.iop.org/1748-9326/12/3/034021)

Environmental Research Letters

LETTER

How does the SST variability over the western North Atlantic Ocean control Arctic warming over the Barents–Kara Seas?

Ok Jung[1], Mi-Kyung Sung[1], Kazutoshi Sato[2], Young-Kwon Lim[3], Seong-Joong Kim[4], Eun-Hyuk Baek[4], Jee-Hoon Jeong[5] and Baek-Min Kim[4,6]

[1] Ewha Womans University-Industry Collaboration Foundation, Seoul Korea
[2] National Institute of Polar Research, Tachikawa, Japan
[3] NASA Goddard Space Flight Center/Global Modeling and Assimilation Office, Goddard Earth Sciences Technology and Research/I. M. Systems Group, Greenbelt, MD, United States of America
[4] Korea Polar Research Institute, Incheon, Korea
[5] Chonnam National University, Gwangju, Korea
[6] Author to whom any correspondence should be addressed.

E-mail: baekmin@gmail.com

Keywords: Arctic warming, Stationary Wave Model, transient eddy vorticity forcing, Western North Atlantic Ocean

Supplementary material for this article is available online

OPEN ACCESS

RECEIVED
21 August 2016

REVISED
8 December 2016

ACCEPTED FOR PUBLICATION
8 February 2017

PUBLISHED
13 March 2017

Abstract

Arctic warming over the Barents–Kara Seas and its impacts on the mid-latitude circulations have been widely discussed. However, the specific mechanism that brings the warming still remains unclear. In this study, a possible cause of the regional Arctic warming over the Barents–Kara Seas during early winter (October–December) is suggested. We found that warmer sea surface temperature anomalies over the western North Atlantic Ocean (WNAO) modulate the transient eddies overlying the oceanic frontal region. The altered transient eddy vorticity flux acts as a source for the Rossby wave straddling the western North Atlantic and the Barents–Kara Seas (Scandinavian pattern), and induces a significant warm advection, increasing surface and lower-level temperature over the Eurasian sector of the Arctic Ocean. The importance of the sea surface temperature anomalies over the WNAO and subsequent transient eddy forcing over the WNAO was also supported by both specially designed simple model experiments and general circulation model experiments.

1. Introduction

The rapid increase in Arctic temperature and retreat of sea ice have been reported and widely discussed in the scientific literatures (Comiso *et al* 2008, Stroeve *et al* 2012, Vihma 2014). The increase in Arctic temperature is most pronounced during early winter (October–December) and is not spatially uniform, but exhibits several particular regional warm cores (Screen and Simmonds 2010) including the Barents–Kara Seas, East Siberian–Chukchi Seas, and northeast Canada and Greenland. Interestingly, the atmospheric warming over each location in the Arctic is known to lead to mid-latitude cooling, but with quite different spatial patterns (Mosley-Thompson *et al* 2005, Cohen *et al* 2012, Francis and Vavrus 2012, Hanna *et al* 2014, Kim *et al* 2014, Mori *et al* 2014, Kug *et al* 2015, Nakanowatari *et al* 2015, Lim *et al* 2016). Therefore, the peculiar recent phenomena called 'Warm Arctic-Cold Continents' (Overland and Wang 2010, Overland *et al* 2015) can be effectively categorized by the regional warm cores in the Arctic.

Although there are many studies on how the above-mentioned regional Arctic warming and reduced sea ice cover over those regions could induce cold winter extremes in mid-latitudes, relatively few studies have been devoted to finding the driving mechanism for those regional Arctic warming events. Recently, a linkage between the oceanic thermal condition of the North Atlantic Ocean and Arctic surface temperature has been suggested (Zhang *et al* 2013, Nakanowatari *et al* 2014, Sato *et al* 2014, Luo *et al* 2016), which is supported by other findings that show both the surface air temperature over the Barents–Kara Seas (BKSAT) and sea surface temperature (SST) over the western North Atlantic Ocean

(WNAO) have rapidly increased in recent decades (Wu *et al* 2012, Pershing *et al* 2015, Saba *et al* 2016). It is also found that the warming over the WNAO is in association with the northward shift of SST front over the Gulf Stream (Minobe *et al* 2008, Wu *et al* 2012).

Among these studies, we revisit Sato *et al* (2014) which provides a close observational link between the Barents–Kara Seas and the WNAO, over which the northern part of the Gulf Stream passes. Using linear baroclinic model experiments, Sato *et al* (2014) suggested that the changes in the local diabatic heating in association with the poleward shift of the Gulf Stream can induce a large-scale circulation pattern travelling into the Arctic inducing significant Arctic warming. However, the linear response shown in figure 5(*d*) of their paper was quite weak and more importantly, missed a possible contribution from the large baroclinic eddy activities over the region, which is amply noted by other studies (Sampe *et al* 2010, Frankignoul *et al* 2011, Sung *et al* 2014). As the transient eddy forcing in the North Atlantic tends to induce the large-scale teleconnection pattern, called the Scandinavian pattern (SCAND), travelling over the north Atlantic and Arctic (Bueh and Nakamura 2007), it is important to take into account baroclinic eddy activities.

In this regard, Sato *et al* (2014)'s study is incomplete, although their finding casts considerable light on the divergent perspectives about 'Warm Arctic-Cold Continents' by revealing that apparent links between the Barents Sea ice cover and cold Eurasian winters form just a sector of a tele-connection pattern that originates remotely in the North Atlantic Gulf Stream region (Simmonds and Govekar 2014). Therefore, it is worthwhile evaluating whether the warming over the WNAO induces a sufficient transient eddy forcing for the large-scale teleconnection pattern over the North Atlantic and Arctic region.

In this study, we aim to provide a more plausible explanation on how the warm SST anomaly in the WNAO sector modulates the Eurasian teleconnections and affects warming over the Arctic, and in particular, the Barents–Kara Sea in early winter. Special attention will be devoted to the role of transient eddy forcing, which was not studied by Sato *et al* (2014). The relative importance of transient eddy forcing to the thermal forcing was assessed by a simple model specially designed to treat each forcing separately. General circulation model experiments were also conducted to support observational findings and simple model results.

2. Datasets and methods

The primary observational dataset used in this study includes Hadley Centre Sea Surface Temperature (HadISST) data with 1° × 1° horizontal resolution (Rayner *et al* 2003) and the re-analysis dataset obtained from the U.S. National Centers for Environmental Prediction (NCEP)/National Center for Atmospheric Research (NCAR), which has a 2.5° × 2.5° horizontal resolution (Kalnay *et al* 1996). Both the daily and monthly mean dataset for the 1979–2013 period were utilized in this study.

In order to investigate distinguishable influences from several independent SST modes of the North Atlantic Ocean separately, Empirical Orthogonal Function (EOF) analysis was applied for early winter (October–December) mean SST anomalies over the North Atlantic Ocean domain (95°W∼15°E, 20.5°N∼88°N). Latitude weighting was applied by multiplying the square root of the cosine prior to the EOF analysis. North's rule of thumb (North *et al* 1982) was used to test the significance of EOF modes. Regression analysis was conducted using the obtained EOF principal component (PC) time series to retrieve the associated circulation patterns.

In this study, interannual variability of surface air temperature over the Atlantic sector of the Arctic region in early winter is represented by the detrended time series of area-averaged BKSAT. The boxed area indicated in figure 1(*a*) was used as the area average.

The stationary wave model (hereafter SWM, Ting and Yu (1998)) was employed to examine the dominant forcing mechanism of stationary Rossby waves. This SWM is the dry dynamical core of a fully nonlinear baroclinic model. The prognostic variables include vorticity, divergence, temperature and log-surface pressure with R30 truncation in the horizontal and L14 vertical levels on sigma coordinates. The main forcings in this model were diabatic heating, convergence of transient eddy vorticity fluxes and transient eddy heat fluxes. The forcing terms can be tested using idealized distribution or diagnosed forcing fields derived from observations. In this study, the latter approach was used (see supplementary information available at stacks.iop.org/ERL/12/034021/mmedia). The three forcing terms can be defined as:

$$TF_{\mathrm{vor}} = -\Delta(\overline{V'\xi'}) \tag{1}$$

$$TF_{\mathrm{temp}} = -\left(\frac{P}{P_0}\right)^{R/C_p}\left[\nabla\cdot\left(\overline{V'\theta'}\right) + \frac{\partial(\overline{\omega'\theta'})}{\partial p}\right] \tag{2}$$

$$Q_1 = \frac{\partial\overline{T}}{\partial t} + \overline{V}\Delta\overline{T} + \overline{\omega}\left(\frac{\partial\overline{T}}{\partial p} - \frac{R\overline{T}}{C_p p}\right) - TF_{\mathrm{temp}} \tag{3}$$

where ξ is the vorticity, V is the horizontal wind, p is pressure, ω is the pressure vertical velocity, and TF_{vor} and TF_{temp} indicate the non-linear transient eddy vorticity flux convergence and transient eddy heat flux convergence, respectively. Q_1 indicates the monthly mean diabatic heating. Note that Q_1 used in this study is different from that in Sato *et al* (2014) because of the

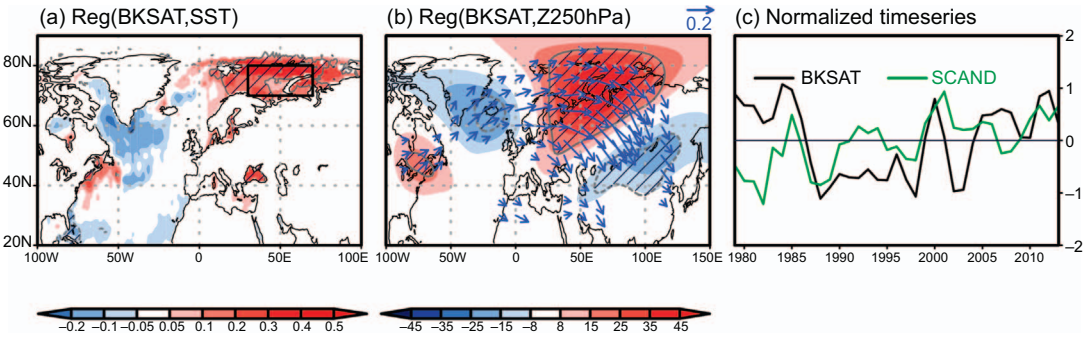

Figure 1. Regression of early winter mean (OND mean) (*a*) SST and (*b*) 250 hPa geopotential height and wave activity on the detrended BKSAT region (30°∼70°E, 70°∼80°N), denoted by the black box in figure 1(*a*). (*c*) Normalized time series of Scandinavian teleconnection index (SCAND, green line) and detrended BKSAT (black line). Hatch represents significance at 95% level of confidence.

existence of TF_{temp} in (3). The bar represents the monthly mean and prime shows the deviation from the monthly mean. Further details of the model equations or information can be found in Ting and Yu (1998) and Wang and Ting (1999).

To investigate the impact of SST warming over the WNAO in a more realistic modelling framework, we used a fully coupled general circulation model (GCM), Climate Model Version 2.1 (CM2.1) developed by the Geophysical Fluid Dynamical Laboratory (GFDL) (Delworth *et al* 2006). As a control run, we conducted climatological equilibrium simulations with 400 ppm CO_2 for 100 years. In a forced simulation, SST over the WNAO region (the box in figure 5(*a*), i.e. 38°N–48°N, 55°W–75°W) was restored toward the prescribed warm SST conditions with 5 day restoring time scale. According to Pershing *et al* (2015), the WNAO region is the highest warming place on the earth and, in the last decade, there was 2 °C increase of SST. Accordingly, we prepared the warm SST condition over the WNAO region by adding the observed SST trend of the recent 11 years (2004–2014) to the climatological SST fields of control run. Note that the model freely evolves except for the boxed region in figure 5(*a*) in the forced run. To estimate the response to the SST forcing over the WNAO, we will analyze differences between the results of the forced run and the control run.

3. Results

3.1. Warming over Barents–Kara Seas and SCAND teleconnection pattern

As suggested by Sato *et al* (2014), during early winter, changes in surface air temperature, especially over the Barents–Kara Seas in the Atlantic sector of the Arctic Ocean, were closely related to changes in SST variability over the WNAO (figure 1(*a*)). In addition to the warming of WNAO, a colder regional SST anomaly over the Labrador Sea was observed in association with the warmer BKSAT constituting the warm–cold–warm tri-polar pattern over a large area of the North Atlantic and European sector of the Arctic Ocean.

The warming over the Barents–Kara Seas in early winter accompanies a well-defined upper-level circulation pattern (figure 1(*b*)). This upper level circulation pattern resembles the EU1 or the SCAND pattern (Barnston and Livezey 1987). In fact, among the teleconnection indices archived at the National Oceanic and Atmospheric Administration (NOAA)/National Center for Environmental Prediction (NCEP)/Climate Prediction Center (CPC), the SCAND index shows the highest correlation with BKSAT. The correlation coefficient between the time series of BKSAT and the early winter mean SCAND index is 0.4, with greater than 95% confidence (figure 1(*c*)).

Interestingly, the wave activity flux vectors (Plumb 1986) in figure 1(*b*) indicate that the wave source region is over the WNAO, not over the Barents–Kara Seas where sea ice loss is pronounced. A large-scale wave pattern with an anticyclonic centre over the WNAO emanates and exhibits a travelling Rossby wave pattern toward eastern Europe, the Barents–Kara Seas, and eventually reaching northeast Asia. In particular, a strong positive upper level geopotential height anomaly over the western North Atlantic region matches the positive SST anomaly over the WNAO. Therefore, the warm SST in figure 1(*a*) over the western North Atlantic region seems to play an important role in the teleconnection. Furthermore, the cold SST anomaly over the Labrador Sea and warm SST anomalies over the Barents–Kara Seas in figure 1 (*a*) also match well with the geopotential height anomalies in figure 1(*b*).

Combining the results displayed in figure 1, we set a series of working hypotheses that can be tested by simple numerical modelling experiments: 1) interannual variability of the BKSAT is, in fact, largely originated from the WNAO. 2) A warmer SST anomaly over the WNAO causes warm temperature anomalies over the Barents–Kara Seas via upper-level planetary wave propagation, similar to SCAND and associated warm advection.

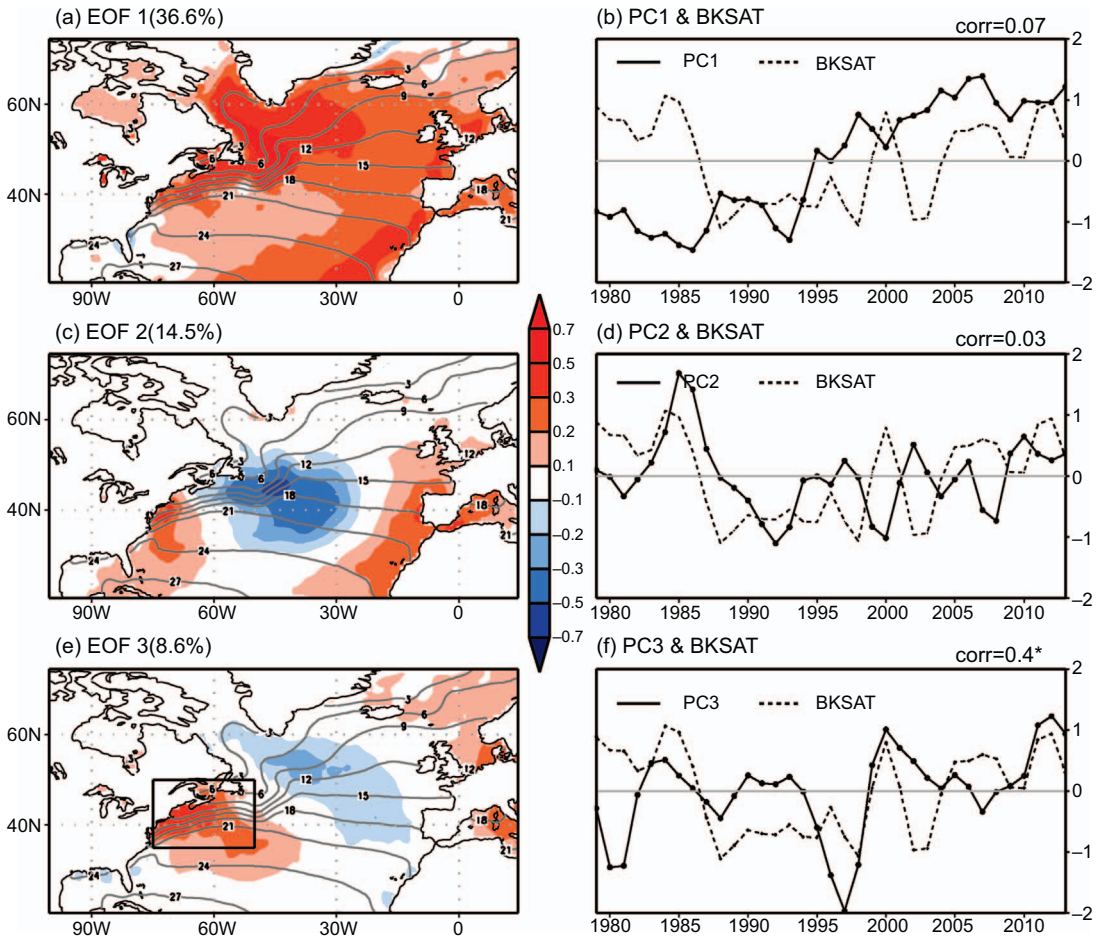

Figure 2. EOF analysis applied to SST anomalies over the North Atlantic Ocean. (*a*) First EOF mode (EOF1) of the early winter mean (OND mean) SST anomaly (shading) and its climatology (contour). (*c*) and (*e*) are the same as (*a*) except for the second and third EOF modes. (*b*) The corresponding PC1 time series for EOF1 (solid line). (*d*) and (*f*) are the same as (*a*) except for the PC time series corresponding to the second and third EOFs. Dashed line in (*b*), (*d*) and (*f*) denotes the time series of detrended BKSAT. Temporal correlation between each PC time series and BKSAT is provided in each panel at the upper-right corner. Box region (75°∼50°W, 35°∼50°N) indicates the WNAO region.

3.2. EOF analysis on North Atlantic SST variabilities

Prior to verifying the above hypotheses, we conducted EOF analysis to determine whether there exists an identifiable North Atlantic SST variability linked to the Arctic warming over the Barents–Kara Seas. The early winter averaged SST anomalies during the 1979–2013 period were decomposed into three dominant modes: the first mode (EOF1) explains 36.6% of the total variance and exhibits a strong linear trend. The spatial pattern of EOF1 shows apparent warming over the entire North Atlantic basin. Although the pattern contains significant SST warming over the Barents–Kara Seas, the correlation between the PC1 and BKSAT is low (0.07). Note that BKSAT is a detrended index.

The second mode explains 14.5% of the variance, and has three centres of action which are located over the western North Atlantic Ocean, the northern North Atlantic Ocean, and the eastern North Atlantic (figure 2(*c*)). The temporal correlation coefficient between the second PC and BKSAT time series is very low (0.03) indicating no significant relationship, as with EOF2 showing no anomalies in the Arctic Sea region. The most similar pattern to the regressed pattern depicted in figure 1(*a*) is described in EOF3, which shows a tripolar pattern with warm SST anomaly over the WNAO; cold over the south of Greenland and Labrador Seas, and warm over the Barents–Kara Seas. The similarity is quite remarkable. As expected by the warm centre over the Barents–Kara Seas in figure 2(*e*), the PC3 time series shows a significant correlation with the BKSAT time series (corr. = 0.4) at 99% confidence level (figure 2(*f*)). The PC3 timeseries also has a high correlation coefficient with the SCAND index (corr. = 0.57) (table 1). According to North's rule of thumb, the three EOF modes are well separated (North *et al* 1982).

It is notable that the SST anomaly over the WNAO lies over the northern edge of the Gulf Stream, which shows a strong SST gradient (see isotherms in figure 2 (*e*)). The warm SST anomaly over this region may represent the poleward shift of the Gulf Stream and intense baroclinic zone. Since it is well-known that the SST gradient associated with the western boundary current is known to be a great source of baroclinicity (Minobe *et al* 2008), it is the source of available

Table 1. Correlation coefficients among the atmospheric teleconnection modes and the PC time series.

	SCAND	EAWR	NAO
PC1	0.1	0.29	0.37
PC2	0.1	0.48[a]	0.02
PC3	0.57[a]	0.10	0.4

[a] Statistically significant at $p < 0.01$.

potential energy for the growth of transient eddies. This leads us to investigate the role of transient eddies in the large-scale teleconnection pattern that links the North Atlantic and the Arctic regions.

3.3. Physical mechanism of Atlantic origin of Arctic warming

Atmospheric circulation features related with the EOF3 of SST variability are depicted in figure 3. Geopotential height anomaly at 250 hPa representing the upper-level circulation features a wave train pattern emanating from the WNAO toward Eurasia across the north-eastern Atlantic and the Barents–Kara Seas (contour in figure 3(*a*)). As expected by the similarity between the SST anomaly regressed on to the BKSAT (figure 1(*a*)) and the EOF third mode (figure 2(*e*)), this upper-level circulation pattern is similar to the SCAND pattern in figure 1 (*b*). The response is equivalent barotropic (contour in figures 3(*a*) and (*b*)) and, therefore, the regressed surface air temperature anomaly (shaded in figure 3 (*a*)) is in general in phase with the upper-level geopotential height anomaly. The significant warming over the Barents–Kara Seas can partly be explained by the enhanced warm advection along the western edge of the anticyclonic anomaly over western Europe induced by this barotropic large-scale anomaly at lower-levels (figure 3(*b*)).

In association with the downstream propagation of SCAND toward East Asia, cold temperature anomalies appear primarily over Central and East Asia, where upper-level cyclonic response dominates (figure 1(*b*)). In this case, the upper-level cyclonic response reduces the thickness of the air column over East Asia and therefore, the column average temperature drops. Combined with the climatologically strong northerly flow in this region, strong cold advection is induced. The warm and cold anomalies explained above resemble 'Warm Arctic-Cold Continents' or 'Warm Arctic-Cold Siberia' pattern (Overland *et al* 2011, Inoue *et al* 2012, Kim *et al* 2014, Mori *et al* 2014, Kug *et al* 2015).

Returning to the North Atlantic, the source region of the wave train seems to lie in the WNAO region (box in figure 2(*e*)). Compared with the EOF3 in figure 2(*e*), this wave activity source region coincides with the warm SST anomaly over the WNAO. Sato *et al* (2014) examined the possible role of the diabatic heating over the WNAO by calculating the apparent heat source and resultant linear stationary eddy response. In this work, we investigated another possibility. The warm SST anomaly over the WNAO can be interpreted as the northward extension of the Gulf Stream (Wu *et al* 2012) indicating northward shift of the ocean front. Since the WNAO region exhibits strong SST gradients as shown in figure 2(*e*), we expect that the warm SST anomaly could alter the activities of synoptic-scale eddies which are sensitive to the temperature gradient and diabatic heat sources (Brayshaw *et al* 2008, Nakamura *et al* 2008). Indeed, the transient eddy activities estimated by the variance of the 300 hPa daily meridional wind anomaly regressed to EOF3 also shifted eastward compared with its climatological position (figure 3(*c*)) and the northward shift of Atlantic sub-polar jet occurred at the same time (figure 3(*d*)). These results are consistent with the previous studies that addressed the importance of the SST gradient in the alteration of transient eddy activities (Sampe *et al* 2010, Frankignoul *et al* 2011, Sung *et al* 2014).

Combined changes in the transient eddy activities and Atlantic sub-polar jet in association with the SST variability over the WNAO hint at the possible role of transient eddy activities on large-scale teleconnection patterns (Bueh and Nakamura 2007, Lim and Kim 2016). To investigate the relative role of transient eddies linked to SST variability over the WNAO, we used the SWM alternatively forced by diabatic heating or transient eddy forcing and estimated the relative importance of each forcing term by comparing the SWM responses forced by each forcing term separately (see supplementary information).

Forcings and associated responses of SWM experiments are represented in figure 4. Within the boxed region of the WNAO, the negative TF_{vor} in figure 4(*a*) was consistent with significant high anomalies shown in figure 1(*b*). Interestingly, the diabatic forcing in figure 4(*c*) and convergence of transient eddy heat flux compensated each other, meaning that the diabatic heating was largely balanced by eddy heat transport.

As noted previously, the WNAO region is a key region of strong SST variability and is associated with the large changes in SST gradient and in storm track. We examined the relative importance of these three forcings in the excitation of large-scale circulation. As shown in figure 4, a major response was obtained with transient eddy vorticity forcing and this forcing reproduced the SCAND wave structure remarkably (compare figure 3(*a*) and figure 4(*a*)). In addition, the wave-like feature in the model response had a high pattern correlation with observed SCAND pattern (0.62). A relatively weaker contribution was obtained from the transient eddy temperature forcing and total diabatic heating forcing. Considering that we only applied the forcing in the restricted region (black box in figure 4), the result is rather surprising and confirms the important role of the storm activities in large-scale teleconnection patterns. These results provide evidence that transient vorticity flux related to the SST

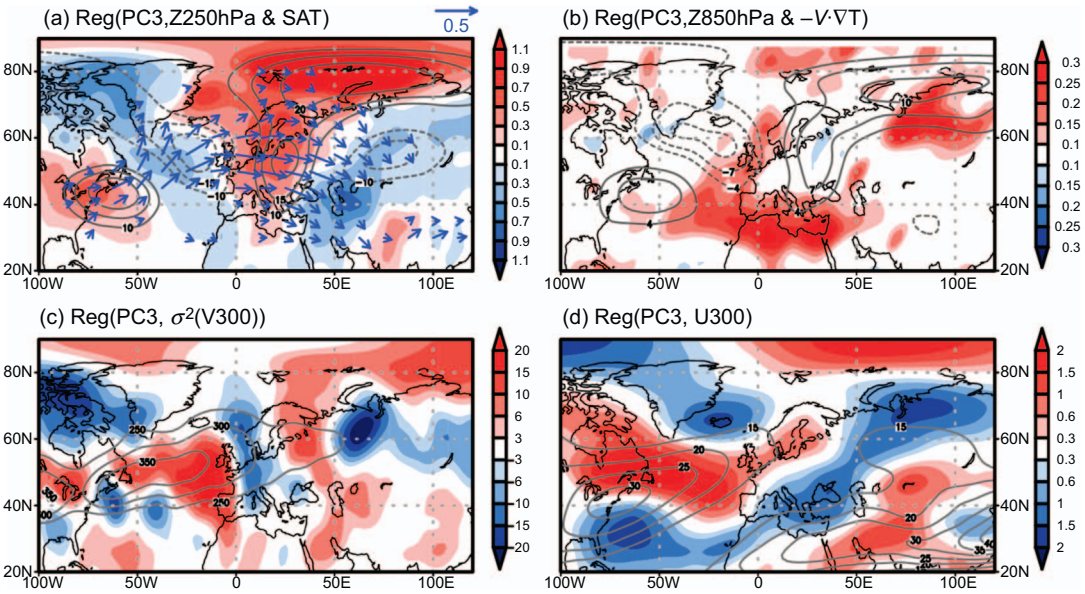

Figure 3. Regression maps constructed using PC3 time series for (*a*) surface air temperature (shading), geopotential height at 250 hPa (contour) and wave activity flux (vector), (*b*) low-level temperature advection anomaly (1000 hPa–850 hPa) (shading) and geopotential height at 850 hPa (contour), (*c*) variance of meridional wind at 300 hPa (shading) and its climatology (contour) and (*d*) zonal wind at 300 hPa (shading) and its climatology (contour).

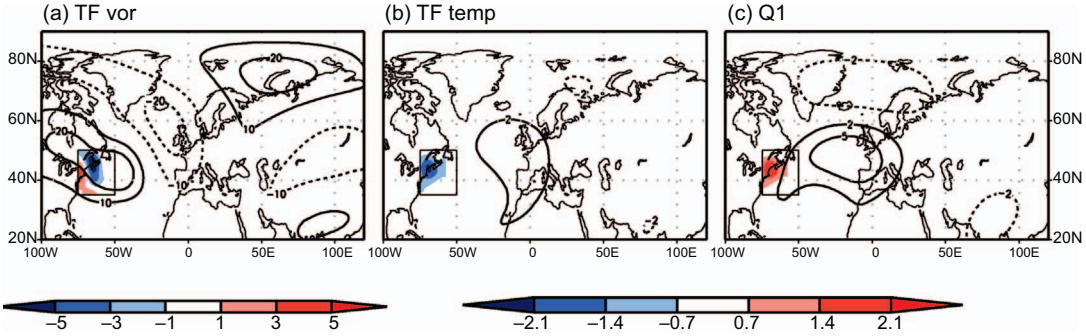

Figure 4. Model response of geopotential height at 300 hPa forced by (*a*) transient eddy vorticity forcing, (*b*) transient temperature forcing and (*c*) diabatic heat source. Forcing is only applied to the boxed region (75°∼50°W, 35°∼50°N). In (*a*), transient eddy vorticity forcing at 300 hPa is represented. Values are normalized by 10^{11}. In (*b*) and (*c*), vertically integrated forcing terms from 925 hPa to 300 hPa are represented and again normalized by 10^{6}. Model streamfunction response is converted to geopotential height by multiplying 10^{-5} divided by gravity.

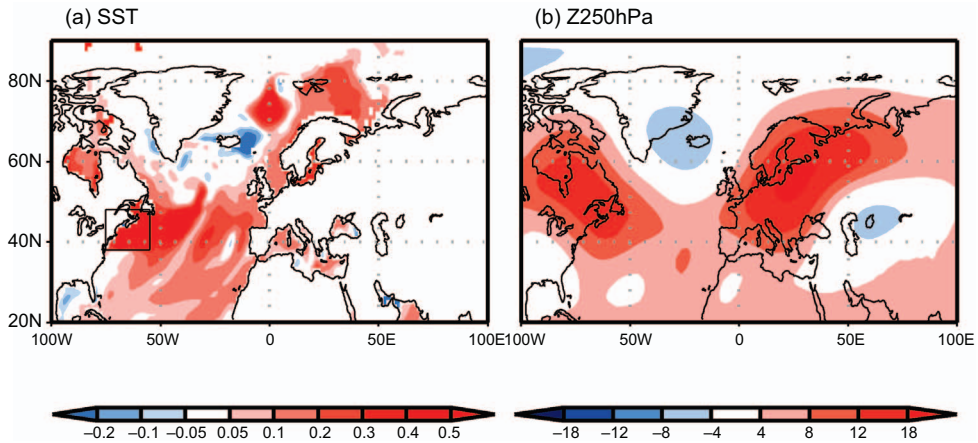

Figure 5. General circulation model (CM2.1) response of (*a*) SST, (*b*) 250 hPa geopotential height during early winter (October–December). The model response is defined as difference between early winter mean of forced run and control run. In forced run, SST is nudged only in the boxed region in (*a*) (75°∼55°W, 38°∼48°N).

interannual variability over the WNAO is a key factor for the SCAND teleconnection pattern.

The last evidence of the importance of SST over the WNAO for the Arctic warming comes from fully coupled model experiments (figure 5). In general, model experiments successfully capture various features depicted in the observational analysis results: Model SST response in figure 5(*a*) shows the warm-cold-warm SST pattern similar to the EOF3 pattern (figure 2(*e*)). Considering that the SST nudging was only applied to the boxed region in figure 5(*a*) in the model simulation. Therefore, the warm SST anomaly over the Barents–Kara Seas was internally generated by the fully coupled model as a response. The upper-level response was also reproduced reasonably well (figure 5 (*b*)). Therefore, the results from the regression analysis (figures 1 and 3) are supported by the fully coupled model experiments.

4. Summary and discussion

Sato *et al* (2014) showed that the poleward shift of the Gulf Stream influences the increase (decrease) of temperature (sea ice extent) over the Barents–Kara Seas and cooling over Eurasia through planetary waves triggered over the Gulf Stream region. In this study, the origins of the planetary waves are investigated in detail.

First, we show that the variability in the surface air temperature over the Barents–Kara Seas is largely controlled by two dominant SST modes in the domain including the North Atlantic Ocean and the Atlantic sector of Arctic Ocean. The warming trends in both the Atlantic Ocean and the Barents–Kara Seas are largely depicted by EOF first mode and this pattern resembles the basin-wide warming pattern. On the other hand, interannual variability is controlled by the tri-polar SST pattern depicted as EOF third mode in this study. The third SST mode represents the poleward shift of the Gulf Stream and accompanying changes in storm track as indicated by Sato *et al* (2014).

Through a simple modelling study using SWM, we concluded that the altered upper-level transient eddy vorticity forcing in association with the changes in the storm track plays a major role in the generation of the SCAND pattern and therefore, plays a bridging role between the North Atlantic Ocean and the Atlantic sector of Arctic in early winter at the interannual time-scale. We could reproduce an upper-level circulation pattern that was very similar to SCAND only with altered transient eddy vorticity forcing in the upper-level.

The surface warm advection along the high pressure center of SCAND at the Barents–Kara Seas, which is essentially barotropic, is an important source of warming of BKSAT. The direct influence of the diabatic heating over the WNAO sector was relatively minor compared to the transient forcing.

Although this study emphasizes the importance of the enhanced transient eddy forcing during the warm period of the WNAO, it should be noted that a large portion of the warming is also contributed by the subsequent reduction of sea ice concentration over the Barents–Kara Seas through the enhanced energy fluxes from the Arctic Ocean (figure A1 in supplementary information). However, in this study, we did not conduct any quantitative assessments on that part since we are only interested in the Atlantic origin of the warming.

It is still unknown why the transient eddy activities show those systematic behaviors responding to the specific SST patterns over the North Atlantic Ocean. To deal with this issue, we need to understand how individual Atlantic storms respond to warm SST over the WNAO by tracking storm intensity and its passage (storm track) along the storm. Both systematic changes in storm intensity and track in association with the particular SST pattern over the North Atlantic should collectively contribute to the monthly-time-scale transient eddy forcing. We are currently investigating this problem by tracking individual Atlantic storms.

Acknowledgments

We thank the two reviewers for their helpful comments. This work is conducted to fulfill the task assigned to the project of Korea Polar Research Institute titled 'Development and Application of the Korea Polar Prediction System (KPOPS) for Climate Change and Disasterous Weather Events'. First author, Jung Ok, is partly supported by 'Development of cloud-precipitation Algorithms' project, funded by ETRI, which is a subproject of 'Development of Geostationary Meteorological Satellite Ground Segment (NMSC-2016-01)' program funded by NMSC (National Meteorological Satellite Center) of KMA (Korea Meteorological Administration). Jee-Hoon Jeong is supported by the Korea Meteorological Administration Research and Development Program (KMIPA2015–2091).

References

Barnston A G and Livezey R E 1987 Classification, seasonality and persistence of low-frequency atmospheric circulation patterns *Mon. Weather Re.* **115** 1083–126

Brayshaw D J, Hoskins B and Blackburn M 2008 The storm-track response to idealized SST perturbations in an Aquaplanet GCM *J. Atmos. Sci.* **65** 2842–60

Bueh C and Nakamura H 2007 Scandinavian pattern and its climatic impact *Q. J. R. Meteorol. Soc.* **133** 2117–31

Cohen J L, Furtado J C, Barlow M A, Alexeev V A and Cherry J E 2012 Arctic warming, increasing snow cover and widespread boreal winter cooling *Environ. Res. Lett.* **7** 014007

Comiso J C, Parkinson C L, Gersten R and Stock L 2008 Accelerated decline in the Arctic sea ice cover *Geophys. Res. Lett.* **35** L01703

Delworth T L *et al* 2006 GFDL's CM2 global coupled climate models. Part I: formulation and simulation characteristics *J. Clim.* **19** 643–74
Francis J A and Vavrus S J 2012 Evidence linking Arctic amplification to extreme weather in mid-latitudes *Geophys. Res. Lett.* **39** L06801
Frankignoul C, Sennéchael N, Kwon Y-O and Alexander M A 2011 Influence of the Meridional shifts of the Kuroshio and the Oyashio extensions on the atmospheric circulation *J. Clim.* **24** 762–77
Hanna E, Fettweis X, Mernild S H, Cappelen J, Ribergaard M H, Shuman C A, Steffen K, Wood L and Mote T L 2014 Atmospheric and oceanic climate forcing of the exceptional Greenland ice sheet surface melt in summer 2012 *Int. J. Climatol.* **34** 1022–37
Inoue J, Hori M E and Takaya K 2012 The role of Barents Sea ice in the wintertime cyclone track and emergence of a warm-arctic cold-Siberian anomaly *J. Clim.* **25** 2561–8
Kalnay E *et al* 1996 The NCEP/NCAR 40-year reanalysis project *Bull. Am. Meteorol. Soc.* **77** 437–71
Kim B-M, Son S-W, Min S-K, Jeong J-H, Kim S-J, Zhang X, Shim T-H and Yoon J-H 2014 Weakening of the stratospheric polar vortex by Arctic sea-ice loss *Nat. Commun.* **5** 4646
Kug J-S, Jeong J-H, Jang Y-S, Kim B-M, Folland C K, Min S-K and Son S-W 2015 Two distinct influences of Arctic warming on cold winters over North America and East Asia *Nat. Geosci.* **8** 759–62
Lim Y K and Kim H D 2016 Comparison of the impact of the Arctic Oscillation and Eurasian teleconnection on interannual variation in East Asian winter temperatures and monsoon *Theor. Appl. Climatol.* **124** 267–79
Lim Y-K, Schubert S D, Nowicki S M, Lee J N, Molod A M, Cullather R I, Zhao B and Velicogna I 2016 Atmospheric summer teleconnections and Greenland ice sheet surface mass variations: Insights from MERRA-2 *Environ. Res. Lett.* **11** 024002
Luo D, Xiao Y, Yao Y, Dai A, Simmonds I and Franzke C L E 2016 Impact of Ural blocking on winter warm arctic-cold Eurasian anomalies. Part I: blocking-induced amplification *J. Clim.* **29** 3925–47
Minobe S, Yoshida-Kuwano A, Komori N, Xie S P and Small R J 2008 Influence of the Gulf Stream on the troposphere *Nature* **452** 206–9
Mori M, Watanabe M, Shiogama H, Inoue J and Kimoto M 2014 Robust Arctic sea-ice influence on the frequent Eurasian cold winters in past decades *Nat. Geosci.* **7** 869–73
Mosley-Thompson E, Readinger C R, Craigmile P, Thompson L G and Calder C A 2005 Regional sensitivity of Greenland precipitation to NAO variability *Geophys. Res. Lett.* **32** L24707
Nakanowatari T, Sato K and Inoue J 2014 Predictability of the Barents Sea ice in early winter: remote effects of oceanic and atmospheric thermal conditions from the North Atlantic *J. Clim.* **27** 8884–901
Nakanowatari T, Inoue J, Sato K and Kikuchi T 2015 Summertime atmosphere-ocean preconditionings for the Bering Sea ice retreat and the following severe winters in North America *Environ. Res. Lett.* **10** 094023
Nakamura H, Sampe T, Goto A, Ohfuchi W and Xie S P 2008 On the importance of midlatitude oceanic frontal zones for the mean state and dominant variability in the tropospheric circulation *Geophys. Res. Lett.* **35** L15709
North G R, Bell T L, Cahalan R F and Moenig F J 1982 Sampling errors in the estimation of empirical orthogonal functions *Mon. Weather Rev.* **110** 669–706
Overland J E and Wang M 2010 Large scale atmospheric circulation changes are associated with the recent loss of Arctic sea ice *Tellus A* **62** 1–9
Overland J E, Wood K R and Wang M 2011 Warm Arctic-cold continents: climate impacts of the newly open Arctic sea *Polar Res.* **30** 15787
Overland J E, Francis J A, Hall R, Hanna E, Kim S-J and Vihma T 2015 The melting Arctic and mid-latitude weather patterns: are they connected? *J. Clim.* **28** 7917–32
Pershing A J *et al* 2015 Slow adaptation in the face of rapid warming leads to collapse of the Gulf of Maine cod fishery *Science* **350** 809–12
Plumb R A 1986 Three-dimensional propagation of Transient Quasi-geostrophic Eddies and its relationship with the Eddy forcing of the time mean flow *J. Atmos. Sci.* **43** 1657–78
Rayner N A, Parker D E, Horton E B, Folland C K, Alexander L V, Rowell D P, Kent E C and Kaplan A 2003 Global analyses of sea surface temperature, sea ice, and night marine air temperature since the late nineteenth century *J. Geophys. Res. Atmos.* **108** 002670
Saba V S *et al* 2016 Enhanced warming of the Northwest Atlantic Ocean under climate change *J. Geophys. Res. Oceans* **121** 118–32
Sampe T, Nakamura H, Goto A and Ohfuchi W 2010 Significance of a Midlatitude SST Frontal Zone in the formation of a Storm Track and an Eddy-Driven Westerly Jet* *J. Clim.* **23** 1793–814
Sato K, Inoue J and Watanabe M 2014 Influence of the Gulf Stream on the Barents Sea ice retreat and Eurasian coldness during early winter *Environ. Res. Lett.* **9** 084009
Screen J A and Simmonds I 2010 Increasing fall-winter energy loss from the Arctic Ocean and its role in Arctic temperature amplification *Geophys. Res. Lett.* **37** L16707
Simmonds I and Govekar P D 2014 What are the physical links between Arctic sea ice loss and Eurasian winter climate? *Environ. Res. Lett.* **9** 101003
Stroeve J C, Kattsov V, Barrett A, Serreze M, Pavlova T, Holland M and Meier W N 2012 Trends in Arctic sea ice extent from CMIP5, CMIP3 and observations *Geophys. Res. Lett.* **39** L16502
Sung M-K, An S-I, Kim B-M and Woo S-H 2014 A physical mechanism of the precipitation dipole in the western United States based on PDO-storm track relationship *Geophys. Res. Lett.* **41** 4719–26
Ting M and Yu L 1998 Steady response to tropical heating in wavy linear and nonlinear baroclinic models *J. Atmos. Sci.* **55** 3565–82
Vihma T 2014 Effects of Arctic sea ice decline on weather and climate: a review *Surv. Geophys.* **35** 1175–214
Wang H and Ting M 1999 Seasonal cycle of the climatological stationary waves in the NCEP-NCAR reanalysis *J. Atmos. Sci.* **56** 3892–919
Wu L *et al* 2012 Enhanced warming over the global subtropical western boundary currents *Nat. Clim. Change* **2** 161–6
Zhang X, He J, Zhang J, Polyakov I, Gerdes R, Inoue J and Wu P 2013 Enhanced poleward moisture transport and amplified northern high-latitude wetting trend *Nat. Clim. Change* **3** 47–51